



CrossMark
 click for updates

Cite this: *RSC Adv.*, 2014, 4, 37679

Characterization and catalytic properties of molybdenum oxide catalysts supported on $ZrO_2-\gamma-Al_2O_3$ for ammoxidation of toluene

Abbas Teimouri,^{*a} Bahareh Najari,^a Alireza Najafi Chermahini,^b Hossein Salavati^a and Mahmoud Fazel-Najafabadi^c

Molybdenum oxide catalysts with MoO_3 loadings ranging from 6.6 to 25 wt% supported on $ZrO_2-\gamma-Al_2O_3$ (1 : 1 wt%) mixed oxide were prepared by a wet impregnation method. The catalytic behavior of catalysts in the toluene ammoxidation reaction was investigated in a lab-scale tube reactor at 400 °C. The catalytic performance of $MoO_3/ZrO_2-\gamma-Al_2O_3$ was dependent on the catalyst compositions and reaction temperature. MoO_3 (20.0 wt%) $ZrO_2-\gamma-Al_2O_3$ exhibited a good toluene oxidation; over this catalyst, the selectivity to benzonitrile reached 67.0% with a toluene conversion of 68.5% at 400 °C, while the selectivity to benzaldehyde was 24.4% with a toluene conversion of 68.5% at 400 °C. The catalysts were characterized by various techniques, such as N_2 sorption, FTIR, SEM and XRD.

Received 22nd July 2014
 Accepted 1st August 2014

DOI: 10.1039/c4ra07435a

www.rsc.org/advances

Introduction

Ammoxidation of alkyl aromatics such as toluene to their corresponding nitriles has been the subject of numerous studies in recent times, because the nitriles are very useful organic intermediates to prepare a good number of industrially important chemicals.^{1,2} The ammoxidation reaction generally refers to the one-step formation of nitrile compounds in a single step by the oxidation of simple olefins, aromatics and heteroaromatics in the presence of oxygen and ammonia in the gas phase.³⁻⁵ Supported molybdenum oxide catalysts are well known and widely investigated as they represent an important group of catalysts for the heterogeneous oxidation and ammoxidation of hydrocarbons.⁶⁻¹⁷

Because pure MoO_3 is relatively volatile, molybdena is almost always used in the presence of a second oxide, on an oxide support such as Al_2O_3 , TiO_2 , ZrO_2 , SiO_2 and MgO .^{6,11,12,14,18-23}

The desirable inherent properties of alumina and zirconia supports can be explored by combination of both supports in a mixed oxide. The $ZrO_2-\gamma-Al_2O_3$ supported catalysts have been found to show better catalytic properties than catalysts supported on pure oxides.^{24,25} The combination of Al_2O_3 and ZrO_2 provides greater mechanical strength, resulting in improved resistance to attrition.^{26,27} In recent times, $ZrO_2-\gamma-Al_2O_3$ based

materials have been employed as catalysts in various catalytic applications.^{28,29} The advantages of $Al_2O_3-ZrO_2$ as a catalyst support include moderate surface area, higher thermal stability and medium acidity. The ammoxidation of toluene^{25,31-53} and other alkyl aromatics^{30,52-63} over various supported metal oxide catalysts has been extensively studied. Iron,⁶⁴⁻⁶⁶ MoO_3/MgF_2 ,⁶⁷ MoO_3/ZrO_2 ,^{68,69} $V_2O_5/ZrO_2-\gamma-Al_2O_3$,^{70,71} $V_2O_5/\gamma-Al_2O_3$,⁷² $Mo-V-P/\gamma-Al_2O_3$,⁷³ vanadium-containing catalysts,^{74,75} Fe_2O_3 -based catalysts,⁷⁶ $ZrO_2-\gamma-Al_2O_3$,⁷⁷ and SiO_2 -supported molybdate catalyst,⁷⁸ have also been used for the preparation of aromatic nitriles.

In the present study, we report the synthesis of benzonitrile by the vapor phase ammoxidation over highly dispersed molybdena catalysts supported on $ZrO_2-\gamma-Al_2O_3$ mixed oxide, as shown in Scheme 1. The catalysts were characterized by X-ray diffraction (XRD), SEM, BET specific surface area and temperature programmed desorption of N_2 .

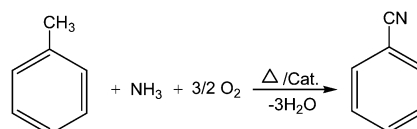
Experimental section

Materials and instruments

Toluene and other agents were purchased from Merck and Aldrich and used without further purification. Products were characterized by spectroscopy data (FTIR, 1H NMR and ^{13}C NMR spectra). NMR spectra were recorded on a Bruker 400 Ultra

^aChemistry Department, Payame Noor University, 81395-671, 19395-3697, Tehran, Isfahan, I. R. of Iran. E-mail: a_teimouri@pnu.ac.ir; a_teimoory@yahoo.com; Fax: +98 31 33521802; Tel: +98 31 33521804

^bDepartment of Chemistry, Isfahan University of Technology, Isfahan, 841543111, Iran
^cMechanical Engineering Department, Payame Noor University, 19395-3697, Tehran, I. R. of Iran



Scheme 1 Catalytic ammoxidation of toluene to benzonitrile.

shield NMR and DMSO-d₆ was used as the solvent. Mass Spectra were recorded on a Shimadzu Gas Chromatograph Mass Spectrometer GCMS-QP5050A/Q P5000 apparatus.

The samples were analyzed by X-ray diffraction (XRD) using Philips X'PERT MPD X-ray diffractometer (XRD) with Cu K α (1.5405 Å). Data sets were collected over the range of 5–90° with a step size of 0.02° and a count rate of 3.0° min⁻¹. The structural morphology of the samples was evaluated using scanning electron microscope (SEM, JEOL, JSM-6300, Tokyo, Japan). A JASCO FT/IR-680 PLUS spectrometer was applied to record IR spectra using KBr pellets. The BET specific surface areas and BJH pore size distribution of the samples were determined by adsorption–desorption of nitrogen at liquid nitrogen temperature using a Series BEL SORP 18.

Catalyst preparation

The MoO₃/ZrO₂ and MoO₃/ γ -Al₂O₃ catalysts were prepared by impregnation of γ -Al₂O₃ or ZrO₂ with a 2 M oxalic solution of ammonium heptamolybdate. The mixture was left in an open vessel with stirring at 60 °C for 24 h to evaporate the excess water. The precursor was dried at 100 °C for 12 h and calcined at 500 °C for 6 h before use.

A series of MoO₃/ZrO₂/ γ -Al₂O₃ catalysts with MoO₃ loadings in the range of 6.6–25.0 wt% were prepared by wet impregnation method. To impregnate MoO₃, the calculated amount of ammonium heptamolybdate was dissolved in 30–40 ml doubly distilled water and reflux at 85–90 °C for 5 h. Then, a few drops of dilute NH₄OH were added to make the solution clear and keep the pH constant (pH = 8). After impregnation, the reaction mixture was added to a 50 ml Pyrex flask. The mixture was irradiated in the water bath of the ultrasonic at 20 kHz for 1 h within the temperature range of 25–30 °C. Then the catalysts were dried at 85–90 °C for about 4 h and calcined at 500 °C for 6 h before use.

Ammonoxidation of toluene

A stainless steel cylindrical micro reactor (i.d. 4.8 cm; a reactor length of 8.55 cm; volume 150 cm³), was charged with toluene (3 ml), 20 mg catalyst and a magnetic stirring bar. The autoclave was purged and filled with NH₃ until the pressure reached 0.75 MPa. Then O₂ was introduced until the total pressure reached to 1.25 MPa. The reaction mixture was stirred at a controlled temperature (400 °C for 2 h). After the reaction, the mixture was filtered. The filtrate was analyzed by GC-MS and GC using benzonitrile as an internal standard. For recycling tests, the catalyst was filtered after the reaction, washed with acetone three times and then with doubly distilled water several times. Then, it was dried at 110 °C, calcined at 400 °C for 4 h, and then used for the next run.

Conversion and selectivity were defined as follows

- C (mol%) = (mol toluene reacted/mol toluene in the feed) \times 100
- Si (mol%) = (mol i formed/mol toluene reacted) \times 100

where i = B, BA, BN.

Results and discussion

XRD analysis

X-ray diffraction (XRD) patterns of the catalysts were obtained using Cu K α radiation (λ = 1.5405 Å). Crystallite size of the crystalline phase was determined from the peak of maximum intensity by using Scherrer formula,⁷⁹ with a shape factor (K) of 0.9, which can be described as: crystallite size = $K\lambda/W \cos \theta$, where $W = W_b - W_s$ and W_b is the broadened profile width of experimental sample and W_s is the standard profile width of reference silicon sample.

Fig. 1A shows the XRD patterns of MoO₃, MoO₃/ZrO₂ and MoO₃/ γ -Al₂O₃ samples. The peaks presented at 2θ = 20–30° are attributed to the pure MoO₃, Fig. 1A(a). The XRD pattern of MoO₃/ZrO₂ showed peaks at 2θ = 30, 50 and 60, which were obviously the characteristics of the tetragonal ZrO₂. The X-ray diffraction pattern of MoO₃/ γ -Al₂O₃ exhibit broad peaks at 2θ = 45 and 66°, which were attributed to γ -Al₂O₃, Fig. 1A(c).

X-ray diffraction patterns of the catalysts with different loadings of molybdena catalysts supported on Al₂O₃–ZrO₂ and calcined at 450 °C are shown in Fig. 1B. The catalysts showed characteristic peaks at 2θ = 32.8, 37.3, 45.9, 62.3 and 66.09° that were related to the support γ -alumina. The sharp diffraction lines at 2θ = 30.4, 51.0 and 60.2° corresponded to the tetragonal ZrO₂ phase. Loading of molybdenum species led to the appearance of new peaks at 2θ = 12.8, 23.9, 22.2, 25.7, 28.5, 34.2 and 39.4°.

FT-IR analysis

The FTIR spectrum for MoO₃ is presented for the range, 350–4000 cm⁻¹ in Fig. 2A(a). The bands at 991, 870, and 491 cm⁻¹, were assigned to the Mo=O stretching mode, the Mo–O–Mo

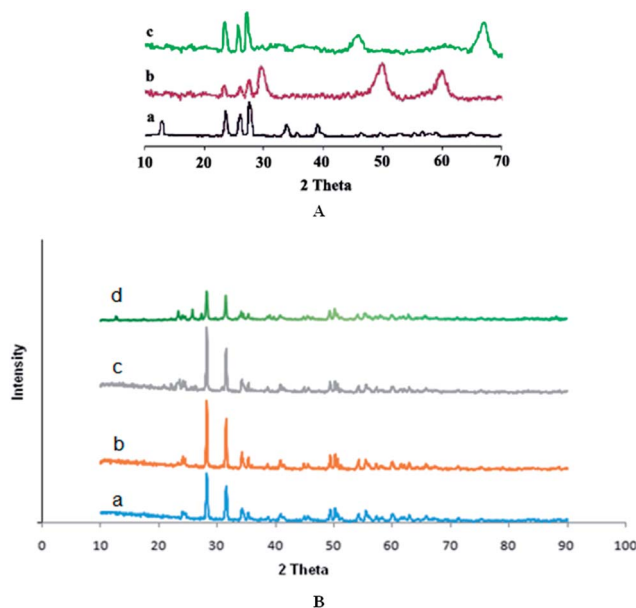


Fig. 1 (A) XRD patterns of (a) MoO₃; (b) MoO₃/ZrO₂; (c) MoO₃/ γ -Al₂O₃. (B) XRD patterns of MoO₃/ZrO₂- γ -Al₂O₃ catalysts with different MoO₃ loadings: (a) 6.6 wt%; (b) 12.5 wt%; (c) 20.0 wt%; (d) 25.0 wt%.

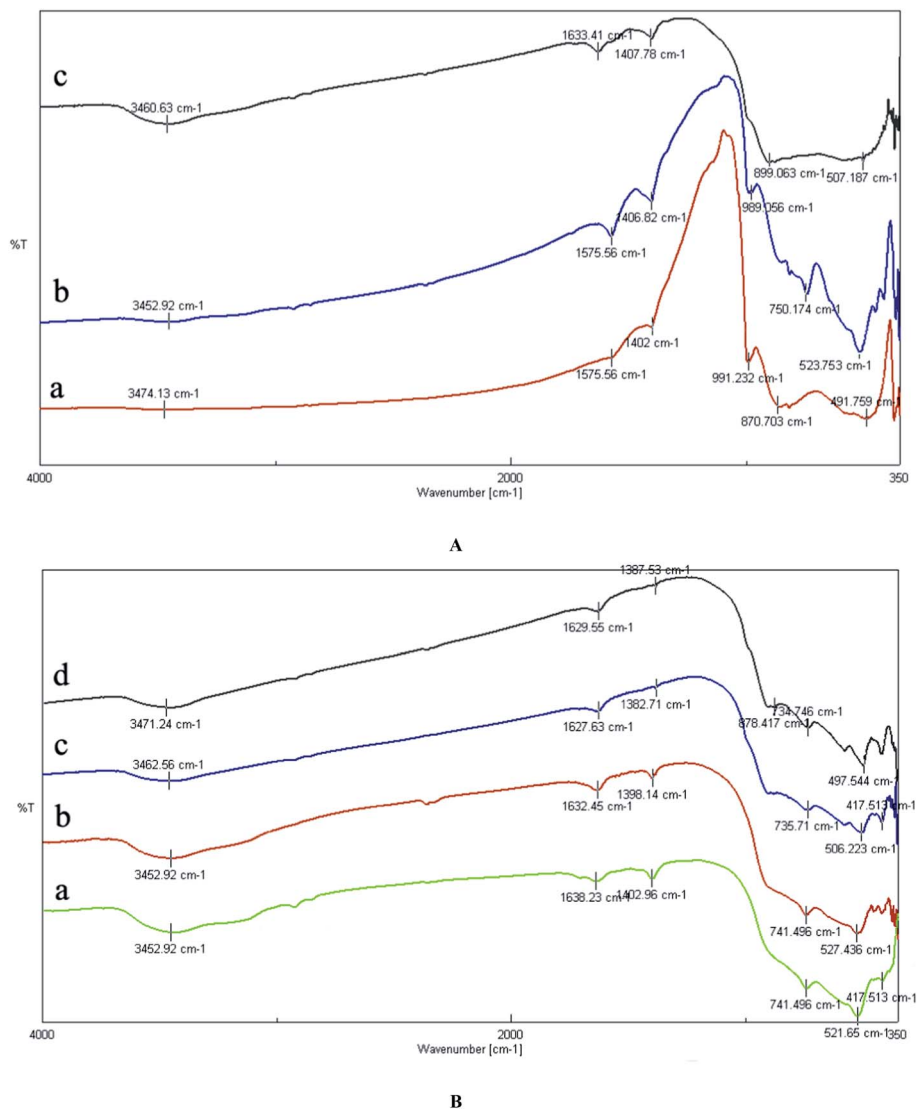


Fig. 2 (A) FTIR spectra of the (a) MoO_3 ; (b) $\text{MoO}_3/\text{ZrO}_2$; (c) $\text{MoO}_3/\gamma\text{-Al}_2\text{O}_3$. (B) FTIR spectra of the $\text{MoO}_3/\text{ZrO}_2\text{-}\gamma\text{-Al}_2\text{O}_3$ catalysts with different MoO_3 loadings: (a) 6.6 wt%; (b) 12.5 wt%; (c) 20.0 wt%; (d) 25.0 wt%.

stretching mode, and MoO_3 vibration mode, respectively. For $\text{MoO}_3/\text{ZrO}_2$ catalyst in Fig. 2A(b), FTIR band at 989 cm^{-1} was due to the $\text{Mo}=\text{O}$ stretching mode of the molybdenum oxide complex bonded to the ZrO_2 surface. Molybdenum oxides species was stabilized through multiple Mo-O-Zr bonds between each molybdenum oxide species and the zirconia surface. The FTIR spectrum for $\text{MoO}_3/\gamma\text{-Al}_2\text{O}_3$ catalyst is shown in Fig. 2A(c). The band at 899 cm^{-1} characterized the stretching mode of the $\text{Mo}=\text{O}$ bond in surface-bound Mo species. These species could be either isolated tetrahedral or octahedral polymolybdate species.

FT-IR spectra of the supports and molybdenum catalysts are shown in Fig. 2B. A broad band in the range of $350\text{--}4000\text{ cm}^{-1}$ appeared for all catalysts related to the MoO_3 species (including the vibrations of Mo-O , bridging oxygen corresponding to Mo-O-Mo). The bands at 878 , 734 and 497 cm^{-1} corresponding to the polymolybdates species. The spectrum in Fig. 2B exhibited bands at $3450\text{--}3760\text{ cm}^{-1}$, typical of the ν

OH bands of alumina hydroxyls. The band at 3764 cm^{-1} was assigned to basic hydroxyl groups bound to a single tetrahedrally coordinated aluminum atom, while the band at 3642 cm^{-1} was due to bridged OH groups shared by an octahedrally and tetrahedrally coordinated aluminum cation. The appearance of the band around 1050 cm^{-1} was typical for γ -alumina due to Al-O vibration mode. On the other hand, bands that appeared at 1632 and 2350 cm^{-1} were related to physisorbed water and OH group free from the interaction of H bonding respectively. There was a strong absorption band at 417 cm^{-1} which could be attributed to the tetragonal zirconia. At higher MoO_3 loading, the bands due to micro-crystallites MoO_3 appeared at 518 , 734 , and 878 cm^{-1} . The increase in the intensity of this band with MoO_3 loading indicated the growth of polymolybdate species. These bands were associated with Mo-O-Al and $\text{Mo}=\text{O}$ bond vibration in aluminum molybdate and crystalline MoO_3 phases, respectively.

SEM analysis

Fig. 3 shows SEM micrographs of catalysts obtained from MoO₃ loadings ranging from 6.6 to 25.0 wt%. Alumina displayed an irregular texture and accumulated aggregates with a variety of particles size. This indicated that the introduction of ZrO₂ into Al₂O₃ largely changed the morphology of the support composites. It can be seen from Fig. 3 that the particles seemed to aggregate to form microspheres. SEM shows a regular texture with small, uniform and dispersed particles.

BET analysis

Fig. 4 shows the N₂ adsorption–desorption isotherms. Surface area was calculated by applying the BET equation to the isotherm.²⁷ The samples were degassed under vacuum at 120 °C for 4 h, prior to adsorption measurement, to evacuate the physisorbed moisture.

The effects of catalyst composition and reaction temperature on the toluene conversion and product distribution for toluene oxidation over MoO₃/ZrO₂-γ-Al₂O₃ are illustrated in Table 1. As shown, the toluene conversion reached a maximum over the catalyst with the MoO₃ loading of 20.0 wt% under each reaction temperature, while the selectivity to the main products fluctuated with the increase of MoO₃ loading.

The MoO₃/ZrO₂/γ-Al₂O₃ catalysts with different MoO₃ contents were evaluated for the ammoxidation of toluene. The ammoxidation of toluene resulted in the formation of benzonitrile as the major product, while benzene and benzaldehyde were formed in very low amounts. The catalysts with the low loading of MoO₃, up to 6.6 wt%, showed moderate activity and when the loading was increased to 20.0 wt%, a substantial increase in activity was observed. The catalyst with 20.0 wt% MoO₃ exhibited the highest activity. With further increase in the active content to 25 wt%, the ammoxidation activity was decreased marginally. The low catalytic activity of 6.6–20.0 wt% MoO₃/ZrO₂/γ-Al₂O₃ catalysts might be because of the less

availability of active MoO₃ compound. With the increase of the reaction temperature, the toluene conversion and the selectivity to benzonitrile and *benzaldehyde* were increased, while the selectivity to benzene was decreased. Over this catalyst, the selectivity to benzonitrile reached to 67.0% with the toluene conversion of 68.5% at 400 °C, while the selectivity to benzonitrile was 58.6% with the toluene conversion of 64.6% at 300 °C. A significant drop in surface area occurred when molybdena loading was increased from 6.6 to 20.0 wt%. Such a decrease might be due to either the blockage of some pores of ZrO₂/γ-Al₂O₃ by mixed oxides formed from the decomposition of molybdate or the solid-state reaction between the supporting oxides and the dispersed active oxides.^{80–82} Table 2 shows the BET surface area values of the catalysts. The surface area and pore volume of the MoO₃/ZrO₂-γ-Al catalysts were in the range of 48–116 m² g⁻¹ and 0.50–0.62 cm³ g⁻¹, respectively. A gradual decrease in surface area was observed for the catalysts with an increase in the loading of molybdena supported on ZrO₂/γ-Al₂O₃, but an increase in the average pore diameters. This phenomenon might be due to two reasons. One refers to MoO₃ particles deposited in the pores of ZrO₂-γ-Al₂O₃ and the blocked part of the small pores.

In addition, the Mo surface density values are measured and data are presented in Table 2. The surface density is defined as the number of Mo atoms per square nanometer BET surface area (Mo atoms nm⁻²). Surface areas decreased only slightly with increasing MoO₃ loading; therefore, the Mo surface density increased almost linearly with increasing MoO₃ concentration. In addition it has been noted that for Mo/Al₂O₃ system, formation of a polymolybdate monolayer on Al₂O₃ at surface densities of 4.8 Mo nm⁻² occur.⁸³ As you can see, the loading 6.6% MoO₃ leads to formation of a molybdate monolayer on mixed oxide surface.

The other relates to the morphology of composite supports changed from big blocks into small particles (observed from SEM image), thereby forming more inter pores between the particles. All samples were mesoporous, with N₂ adsorption–desorption isotherms of type IV according to the IUPAC classification. Such isotherms are shown in Fig. 4, which shows the case of a bare support taken as a representative example for 20.0 wt% MoO₃/ZrO₂-γ-Al₂O₃ catalyst.

One of the most important advantages of heterogeneous catalysis over the homogeneous counterpart is the possibility of reusing the catalyst by simple filtration, without loss of activity. The recovery and reusability of the catalyst were investigated in the product formation. After completion of the reaction, the catalyst was separated by filtration, washed first 3 times with 5 ml acetone and then with doubly distilled water several times, dried at 110 °C and calcined at 400 °C for 4 h. Then the recovered catalyst was used in the next run. The results of three consecutive runs showed that the catalyst could be reused several times without any significant loss of its activity (see Fig. 5).

It is generally accepted that the reaction proceeds by the adsorption of toluene on the catalyst surface through the formation of a π-complex with a Lewis site of the catalyst; furthermore, we should consider H abstraction of a benzylic H-atom to form a methylene-like species with parallel formation

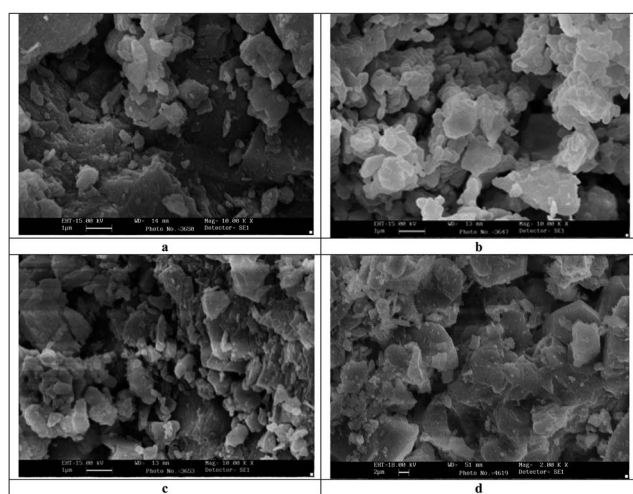


Fig. 3 SEM images of the molybdate supported catalysts (a) 6.6 wt% MoO₃/ZrO₂-γ-Al₂O₃, (b) 12.5 wt% MoO₃/ZrO₂-γ-Al₂O₃, (c) 20.0 wt% MoO₃/ZrO₂-γ-Al₂O₃, (d) 25.0 wt% MoO₃/ZrO₂-γ-Al₂O₃.

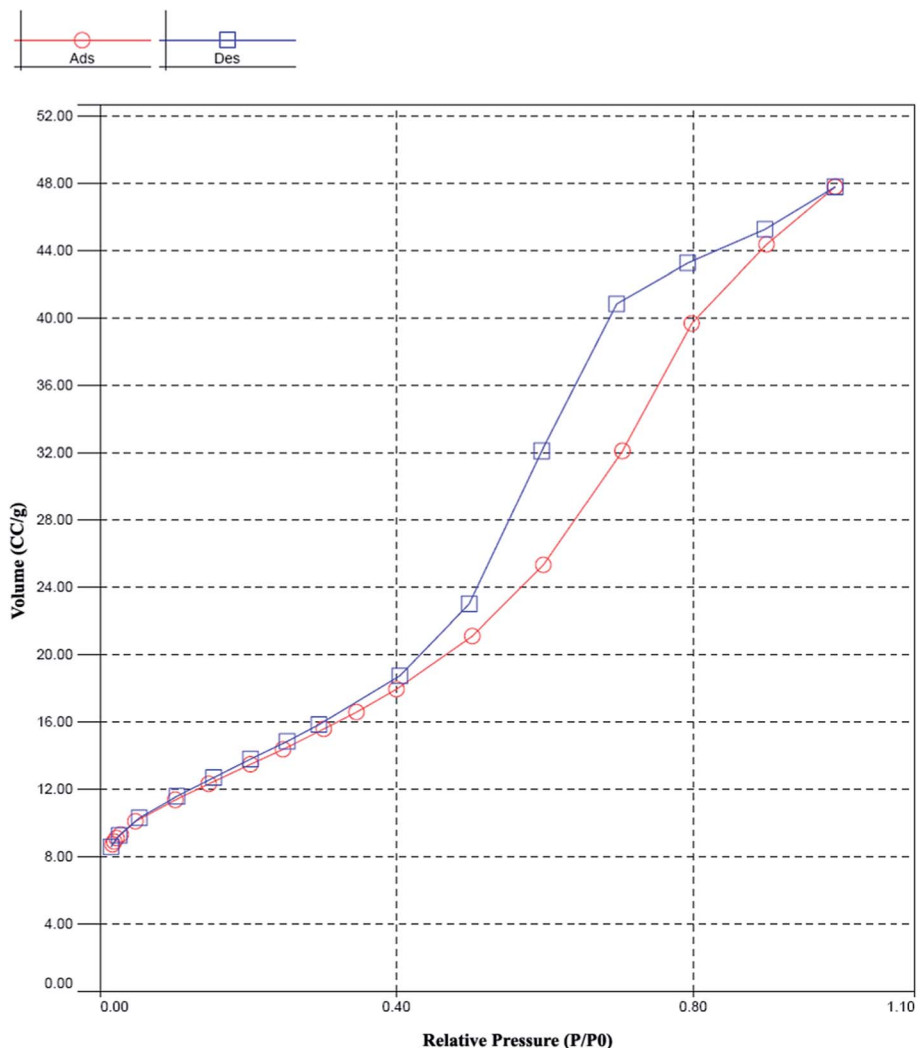


Fig. 4 N_2 adsorption–desorption isotherm of the MoO_3 (20.0 wt%)/ ZrO_2 - γ - Al_2O_3 .

Table 1 Effect of MoO_3 content in the support on the catalyst activity and product selectivity of different MoO_3/ZrO_2 - γ - Al_2O_3 catalysts for toluene ammoxidation

| MoO ₃ loading | T (°C) | Toluene conversion (%) | Product selectivity (%) | | |
|--------------------------|--------|------------------------|-------------------------|---------|--------------|
| | | | Benzonitrile | Benzene | Benzaldehyde |
| 6.6% | 200 | 28.6 | 40.7 | ≤1 | 20.5 |
| | 300 | 44.5 | 46.2 | 1.3 | 23.7 |
| | 400 | 44.2 | 63.5 | 2 | 24.4 |
| 12.5% | 200 | 32.5 | 46.3 | ≤1 | 20.5 |
| | 300 | 48.4 | 50.4 | 1.3 | 23.7 |
| | 400 | 56.6 | 66.4 | 2 | 24.4 |
| 20.0% | 200 | 44.2 | 40.3 | 1.3 | 23.7 |
| | 300 | 64.6 | 58.6 | 2 | 24.4 |
| | 400 | 68.5 | 68 | ≤1 | 24.4 |
| 25.0% | 200 | 30.3 | 35.9 | ≤1 | 20.5 |
| | 300 | 43.7 | 47.5 | 1.3 | 23.7 |
| | 400 | 48.6 | 67.6 | 2 | 24.2 |

of water, partial oxidation, N-insertion and subsequent rearrangements of the chemisorbed activated surface species, which was converted to an adsorbed imine, and desorption of

the so formed benzonitrile, which was followed by oxidative reconstruction of the catalyst surface (Fig. 6). A similar mechanism has been proposed for this reaction.⁸⁴

Table 2 Nitrogen adsorption characteristics of molybdate supported catalysts

| Catalyst | BET surface area (m ² g ⁻¹) | Surface density Mo/nm ² | Pore volume (cm ³ g ⁻¹) | Average pore diameter (nm) |
|--|--|------------------------------------|--|----------------------------|
| 6.6% MoO ₃ /ZrO ₂ -γ-Al ₂ O ₃ | 116.26 | 2.37 | 0.78 | 6.22 |
| 12.5% MoO ₃ /ZrO ₂ -γ-Al ₂ O ₃ | 78.13 | 6.69 | 0.74 | 6.23 |
| 20.0% MoO ₃ /ZrO ₂ -γ-Al ₂ O ₃ | 66.32 | 12.61 | 0.68 | 6.25 |
| 25.0% MoO ₃ /ZrO ₂ -γ-Al ₂ O ₃ | 48.46 | 21.57 | 0.64 | 6.34 |

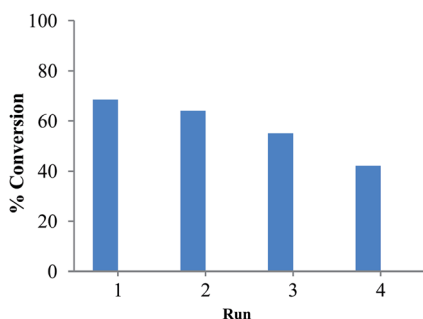


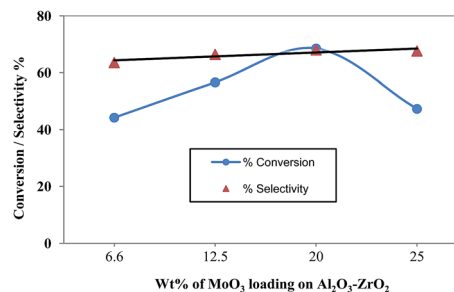
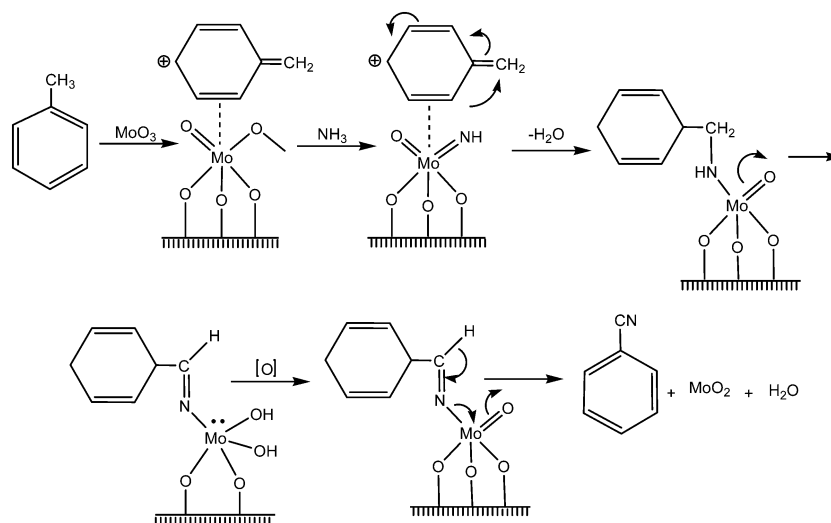
Fig. 5 The results obtained from catalyst reuse in the product formation.

This was also reflected in the catalytic activity of these catalysts. Conversion of toluene to benzonitrile was increased continuously with molybdena loading up to 20.0 wt%. It indicated that the moderate and weak acidic sites played an important role in the ammoxidation of toluene.

The results of ammoxidation of toluene on various MoO₃/ZrO₂-γ-Al₂O₃ catalysts at 400 °C are plotted in Fig. 7. The conversion and selectivity were increased with an increase in MoO₃ loading up to 20.0 wt% and beyond this loading, the activity was decreased slightly due to the formation of MoO₃-crystallites on the surface of ZrO₂-γ-Al₂O₃ support. The increase in the ammoxidation activity of the catalysts might be attributed

to the increase in the number of sites on the active molybdena phase, which could be increased with the increase in molybdena content on the surface of the support. The surface properties and catalytic activity results of 20.0 wt% MoO₃ supported on mixed oxide alumina-zirconia catalysts have been compared in Table 2. It clearly shows that molybdena was well dispersed on MoO₃/ZrO₂-γ-Al₂O₃ support, with more acidic sites per m² surface of the support.

Thus, it can be inferred that 20.0 wt% MoO₃/ZrO₂-γ-Al₂O₃ catalyst can be more active in ammoxidation reaction compared to a time when it is supported on alumina-zirconia catalysts.

Fig. 7 Ammoxidation of toluene over various MoO₃/ZrO₂-Al₂O₃ catalysts (reaction temperature of 400 °C).Fig. 6 A plausible mechanism for toluene ammoxidation over MoO₃/ZrO₂-γ-Al₂O₃ catalysts.

Benzonitrile characterization

FTIR (KBr, cm^{-1}): 3116, 3064, 2256, 1662, 1098, 625 cm^{-1} ; ^1H NMR (400 MHz, DMSO- d_6): δ 7.383–7.412 (m, 2H), 7.518–7.561 (m, 3H); ^{13}C NMR (100 MHz, DMSO- d_6): δ 112.30 (1C), 118.82 (1C), 129.16 (2C), 132.05 (2C), 132.82 (1C); ESI MS (m/z): 103.08 (M^+).

Conclusions

The catalyst $\text{MoO}_3/\text{ZrO}_2\text{-}\gamma\text{-Al}_2\text{O}_3$ exhibited excellent catalytic performance in toluene ammoxidation with benzonitrile as the main product. The $\text{Al}_2\text{O}_3\text{-ZrO}_2$ binary oxide was found to be an interesting support to investigate the dispersion of molybdenum oxide and catalytic properties. The catalytic performance of $\text{MoO}_3/\text{ZrO}_2\text{-}\gamma\text{-Al}_2\text{O}_3$ was dependent on the catalyst compositions and reaction temperature. Increasing the MoO_3 loading from 6.6 to 25.0 wt% enhanced the activity of the catalyst. Above 20.0 wt%, however, it led to inactivity and performance failure of the catalyst. Over this catalyst, the selectivity to benzonitrile reached 67.0% with the toluene conversion of 68.5% at 400 °C, while the selectivity to benzonitrile was 58.6% with the toluene conversion of 64.6% at 300 °C.

Conflict of interest

The authors declare no competing financial interest.

Acknowledgements

The authors would like to thank the Iranian National Science Foundation (INSF) for financial support of this work. Supports from Isfahan research council at Payame Noor University and the help from Isfahan University of technology are gratefully acknowledged.

Notes and references

- V. M. Bondareva, T. V. Andrushkevich, E. A. Paukshtis, N. A. Paukshtis, A. A. Budneva and V. N. Parmon, *J. Mol. Catal. A: Chem.*, 2007, **269**, 240–245.
- R. G. Rizayev, E. A. Mamedov, V. P. Vislovskii and V. E. Sheinin, *Appl. Catal., A*, 1992, **83**, 103–140.
- R. K. Grasselli and M. A. Tenhover in *Handbook of Heterogeneous Catal*, ed. G. Ertl, H. Knözinger, F. Schth and J. Weitkamp, Wiley-VCH, Weinheim, 2008, pp. 3489–3517.
- A. Martin and B. Lcke, *Catal. Today*, 2000, **57**, 61–70.
- R. K. Grasselli, *Catal. Today*, 1999, **49**, 141–153.
- G. Tsilomelekis, A. Christodoulakis and S. Boghosian, *Catal. Today*, 2007, **127**, 139–147.
- G. C. Behera, K. Parida, N. F. Dummer, G. Whiting, N. Sahu, A. F. Carley, M. Conte, G. J. Hutchings and J. K. Bartley, *Catal. Sci. Technol.*, 2013, **3**, 1558–1564.
- S. T. Oyama, R. Radhakrishnan, M. Seman, J. N. Kondo, K. Domen and K. Asakura, *J. Phys. Chem. B*, 2003, **107**, 1845–1852.
- R. Nie, J. Shi, S. Xia, L. Shen, P. Chen, Z. Hou and F.-S. Xiao, *J. Mater. Chem.*, 2012, **22**, 18115–18118.
- E. V. Ishchenko, T. V. Andrushkevich, G. Ya. Popova, T. Yu. Kardash, A. V. Ishchenko, L. S. Dovlitova and Yu. A. Chesalov, *Appl. Catal., A*, 2014, **476**, 91–102.
- X. B. Ma, J. L. Gong, S. P. Wang, N. Gao, D. L. Wang, X. Yang and F. He, *Catal. Commun.*, 2004, **5**, 101–106.
- S. Zhang, Q. Zhong, W. Zhao and Y. Li, *Chem. Eng. J.*, 2014, **253**, 207–216.
- G. M. Dharand, B. N. Srinivas, M. S. Ranaand, M. Kumarand and S. K. Maity, *Catal. Today*, 2003, **86**, 45–60.
- K. V. R. Chary, K. R. Reddy, G. Kishan, J. W. Niemantsverdriet and G. Mestl, *J. Catal.*, 2004, **226**, 283–291.
- Catal. from A to Z: a Concise Encyclopedia*, ed. B. Cornils, W. A. Herrmann, M. Muhler and C.H. Wong, Wiley-VCH, Weinheim, Germany, 3rd edn, 2007.
- M. L. Pacheco, J. Soler, A. Dejoz, J. M. Lopez Nieto, J. Herguido, M. Menendez and J. Santamaria, *Catal. Today*, 2000, **61**, 101–107.
- J. E. Miller, N. B. Jackson, L. Evans, A. G. Sault and M. M. Gonzates, *Catal. Lett.*, 1999, **12**, 147–152.
- R. Radhakrishnan, C. Reed, S. T. Oyama, M. Seman, J. N. Kondo, K. Domen, Y. Ohminami and K. Asakura, *J. Phys. Chem. B*, 2001, **105**, 8519–8530.
- K. Y. S. Ng and E. Gulari, *J. Catal.*, 1985, **92**, 340–354.
- Y. S. Jin, A. Auroux and J. C. Vedrine, *J. Chem. Soc., Faraday Trans.*, 1989, **83**, 4179–4191.
- H. Miyata, S. Toukuda, T. Ono and F. Hatayama, *J. Chem. Soc., Faraday Trans.*, 1990, **86**, 2291.
- T. Ono, H. Miyata and Y. Kubokaw, *J. Chem. Soc., Faraday Trans.*, 1987, **83**, 1761–1770.
- H. Miyata, S. Toukuda, T. Ono, T. Othno and F. Hatayama, *J. Chem. Soc., Faraday Trans.*, 1990, **86**, 3679–3682.
- M. Sanati and A. Andersson, *Appl. Catal., A*, 1993, **106**, 51–72.
- Y. Murakami, M. Niwa, T. Hattori, S. Osawa, I. Igushi and H. Ando, *J. Catal.*, 1977, **49**, 83–91.
- A. Sahibed-Dine, B. Bouanis, K. Nohair and M. Bensitel, *Ceram. Int.*, 2002, **28**, 159–164.
- S. C. Farmer and A. Sayir, *Eng. Fract. Mech.*, 2002, **69**, 1015–1024.
- C. Larese, J. M. Campos-Martin, J. J. Calvino, G. Blanco, J. L. G. Fierro and Z. C. Kang, *J. Catal.*, 2002, **208**, 467–478.
- S. Castillo, M. Moran-Pineda and R. Gomez, *Catal. Commun.*, 2001, **2**, 295–300.
- R. G. Rizayev, E. A. Mamedov, V. P. Vislovskii and V. E. Sheinin, *Appl. Catal., A*, 1992, **83**, 103–140.
- M. Niwa, H. Ando and Y. Murakami, *J. Catal.*, 1977, **49**, 92–96.
- Y. Murakami, H. Ando and M. Niwa, *J. Catal.*, 1981, **67**, 472–474.
- M. Niwa, M. Sago, H. Ando and Y. Murakami, *J. Catal.*, 1981, **69**, 69–76.
- M. Niwa and Y. Murakami, *J. Catal.*, 1982, **76**, 9–16.
- P. Cavalli, F. Cavani, I. Manenti and F. Trifiro, *Ind. Eng. Chem. Res.*, 1987, **26**, 639–647.
- P. Cavalli, F. Cavani, I. Manenti, F. Trifiro and M. El-Sawi, *Ind. Eng. Chem. Res.*, 1987, **26**, 804–810.

- 37 G. Busca, F. Cavani and F. Trifiro, *J. Catal.*, 1987, **106**, 471–482.
- 38 J. C. Otamiri and A. Andersson, *Catal. Today*, 1988, **3**, 211–222.
- 39 J. C. Otamiri and A. Andersson, *Catal. Today*, 1988, **3**, 223–234.
- 40 A. Andersson and S. Hansen, *J. Catal.*, 1988, **114**, 332–346.
- 41 M. Sanati and A. Andersson, *Ind. Eng. Chem. Res.*, 1991, **30**, 312–320.
- 42 M. Sanati and A. Andersson, *Ind. Eng. Chem. Res.*, 1991, **30**, 320–326.
- 43 M. Sanati, L. R. Wallenberg, A. Andersson, S. Jansen and Y. Tu, *J. Catal.*, 1991, **32**, 128–144.
- 44 S. Jansen, Y. Tu, M. J. Palmieri, M. Sanati and A. Andersson, *J. Catal.*, 1992, **138**, 79–89.
- 45 M.-D. Lee, W.-S. Chen and H.-P. Chiang, *Appl. Catal., A*, 1993, **101**, 269–281.
- 46 M. Sanati, A. Andersson, L. R. Wallenberg and B. Rebenstorf, *Appl. Catal., A*, 1993, **106**, 51–72.
- 47 A. Andersson, S. L. T. Andersson, G. Centi, R. K. Grasselli, M. Sanati and F. Trifiro, *Appl. Catal., A*, 1994, **113**, 43–57.
- 48 S. J. Kulkarni, R. Ramachandra Rao, M. Subrahmanyam, A. V. Rama Rao, A. Sarkani and L. Guczi, *Appl. Catal., A*, 1996, **139**, 59–74.
- 49 K. V. R. Chary, K. R. Reddy, T. Bhaskar and G. V. Sagar, *Green Chem.*, 2002, **4**, 206–209.
- 50 C. P. Kumar, K. R. Reddy, V. V. Rao and K. V. R. Chary, *Green Chem.*, 2002, **4**, 513–516.
- 51 K. Smeykal, K.-K. Moll, E. Heyner, K. Pelzing and U. Schattenholz, UK Patent 1124457, 1968.
- 52 *Handbook of Heterogeneous Catal*, ed. R. K. Grasselli, G. Ertl, H. Knoezinger and J. Weitkamp, Wiley, Weinheim, 1997, vol. 5, pp. 2303–2379.
- 53 M. V. Landau, M. L. Kaliya and M. Herskowitz, *Appl. Catal., A*, 2001, **208**, 21–34.
- 54 (a) K. V. Narayana, A. Martin, U. Bentrup, B. Lücke and J. Sans, *Appl. Catal., A*, 2004, **270**, 57–64; (b) N. Dropka, Q. Smejkal, V. N. Kalevaru and A. Martin, *J. Catal.*, 2006, **240**, 8–17.
- 55 N. Dropka, Q. Smejkal, V. N. Kalevaru and A. Martin, *Appl. Catal., A*, 2008, **349**, 125–132.
- 56 A. Martin, V. N. Kalevaru and Q. Smejkal, *Catal. Today*, 2010, **157**, 275–279.
- 57 A. B. Azimov, V. P. Vislovskii, E. A. Mamedov and R. G. Rizayev, *J. Catal.*, 1991, **127**, 354–360.
- 58 G. Centi, *Appl. Catal., A*, 1996, **147**, 267–298.
- 59 R. K. Grasselli, *Catal. Today*, 1999, **49**, 141–153.
- 60 A. Martin and B. Lücke, *Catal. Today*, 2000, **57**, 61–70.
- 61 A. Martin, N. V. Kalevaru, B. Lucke and J. Sans, *Green Chem.*, 2002, **4**, 481–485.
- 62 A. Martin, U. Bentrup and G.-U. Wolf, *Appl. Catal., A*, 2002, **227**, 131–142.
- 63 A. Martin, V. N. Kalevaru and B. Lucke, *Catal. Today*, 2003, **78**, 311–317.
- 64 P. Nagaraju, N. Lingaiah, M. Balaraju and P. S. Sai Prasad, *Appl. Catal., A*, 2008, **339**, 99–107.
- 65 P. Nagaraju, Ch. Srilakshmi, N. Pasha, N. Lingaiah, I. Suryanarayana and P. S. Sai Prasad, *Catal. Today*, 2008, **131**, 393–401.
- 66 M. D. Allen, G. J. Hutchings and M. Bowker, *Appl. Catal., A*, 2001, **217**, 33–39.
- 67 J. Haber and M. Wojciechowska, *Catal. Lett.*, 1991, **10**, 271–278.
- 68 T. Bhaskar, K. R. Reddy, C. P. Kumar, M. R. V. S. Murthy and K. V. R. Chary, *Appl. Catal., A*, 2001, **211**, 189–201.
- 69 K. V. R. Chary, K. R. Reddy, G. Kishan, J. W. Niemantsverdriet and G. Mestl, *J. Catal.*, 2004, **226**, 283–291.
- 70 K. V. R. Chary, C. P. Kumar, P. V. R. Rao and V. V. Rao, *Catal. Commun.*, 2004, **5**, 479–484.
- 71 Y. Zhao, Z. Qin, G. Wang, M. Dong, L. Huang, H. Wua, W. Fanand and J. Wang, *Fuel*, 2013, **104**, 22–27.
- 72 Y. Jeon, S. W. Row, A. Dorjgotov, S. D. Lee, K. Oh and Y. G. Shul, *Korean J. Chem. Eng.*, 2013, **30**(5), 1–5.
- 73 B. Hari Babu, G. Parameswaram, A. Sri Hari Kumar, P. S. Sai Prasad and N. Lingaiah, *Appl. Catal., A*, 2012, 445–446.
- 74 A. Martin and B. Lucke, *Catal. Today*, 2000, **57**, 61–70.
- 75 A. Martin, U. Bentrup and G. U. Wolf, *Appl. Catal., A*, 2002, **227**, 131–142.
- 76 E. Rombi, I. Ferino, R. Monaci, C. Picciau, V. Solinas and R. Buzzoni, *Appl. Catal., A*, 2004, **266**, 73–79.
- 77 K. V. R. Chary, C. P. Kumara, D. Naresh, T. Bhaskar and Y. Sakata, *J. Mol. Catal. A: Chem.*, 2006, **243**, 149–157.
- 78 M. A. de Boer, A. J. A. Van Dillen, D. C. A. Koningsberger, J. W. A. Geus, M. A. A. Vuurman and I. E. A. Wachs, *Catal. Lett.*, 1990, **11**, 227–240.
- 79 B. D. Cullity and S. R. Stock, *Elements of X-ray Diffraction*, Prentice Hall, Upper Saddle River, NJ, 3rd edn, 2001, p. 388.
- 80 K. V. R. A. Chary, C. P. A. Kumar, P. V. R. A. Rao and V. V. A. Rao, *Catal. Commun.*, 2004, **5**, 479–484.
- 81 Y. A. Murakami, M. A. Niwa, T. A. Hattori, S. i. A. Osawa, I. A. Igushi and H. A. Ando, *J. Catal.*, 1977, **49**, 83–91.
- 82 M. A. Sanati, A. A. Andersson, L. R. A. Wallenberg and B. A. Rebenstorf, *Appl. Catal., A*, 1993, **106**, 51–72.
- 83 Y. Chen and L. F. Zheng, *Catal. Lett.*, 1992, **12**, 51–62.
- 84 J. A. Haber and M. A. Wojciechowska, *J. Catal.*, 1988, **110**, 23–36.